International Journal of Pure and Applied Mathematics

Volume 21 No. 3 2005, 277-291

BISTABILITY OF V-SHAPE OF NONLINEAR ATOMIC SYSTEM WITH PHASE-SENSITIVE SOURCE

H.A. Batarfi

Department of Mathematics
Faculty of Science
King Abdul Aziz University (Women' Section)
P.O. Box 41101, Jeddah, 21521, KINGDOM OF SAUDI ARABIA
e-mail: hbatarfi@kaau.edu.sa

Abstract: The input-output problem of a bistable behaviour of a nonlinear (atomic) medium of 3-level V-shaped structure in a ring cavity configuration driven by a coherent field and in contact with a phase-sensitive (squeezed vacuum) reservoir environment is modelled and treated computationally in the steady state region. The interplay of the (quantum) interference effect (associated with the 3-level structure) and the effect of the phase-sensitive reservoir is investigated in detail.

AMS Subject Classification: 37N20
Key Words: bistability, three-level atoms, V-shape atomic system, Maxwell-Bloch equations

1. Introduction

The recent mathematical and computational interest in the topic of optical communications is due to the technological advances in phenomena like: optical bistability (OB), optical fibres, optical computers and quantum computers [1-7]. In addition, the availability of light field sources of lesser (quantum) noise (called phase-sensitive sources or squeezed light) has encouraged researchers to probe various (classical or quantum) systems as this provides finer measurements and predict new effects in radiation-matter interactions [8, and references therein].

Received: February 22, 2005

Specifically, the bistable behaviour of a simple dissipative 2-level atomic structure placed in an optical ring cavity is well studied since the first paper of Bonifacio and Lugiato in 1976, see [9]. The dissipative process of the atomic system is treated as "environmental interaction" with a reservoir of large number of harmonic oscillators at zero temperature (i.e. the state of the surrounding radiation field is in the normal vacuum (NV) state). Recent investigation [10-14] of the 2-level OB system where the environmental reservoir is in the squeezed vacuum (SV) state, rather than the NV state, provided rich of informations, among which: lower critical value for the atomic cooperative parameter [13], novel "phase switching effect" [11] of various shapes ("isola" and "mushroom" structure [13, 14]).

In the present work, we extend our earlier study [13, 14] to the case of OB system of 3-level atomic energy structure of V-shape in interaction with SV reservoir. The 3-level atomic structure is of recent current theoretical (and experimental) investigation because of the important role of the quantum interference effect that takes place between the two-decay channels associated with the two-upper levels. Also, the 3-level atomic structure is important to induce highly-dispersive media and "lasing" action without atomic inversion [15, and references therein].

In this final report of the funded project we report the model Bloch equations for the atomic variables for the 3-level V-shape of atomic structure in interaction with environmental SV reservoir (which was reported in the first report) together with the computational investigation of the steady state atomic variables and the characteristic steady state input/output relation. The major investigation is to display the role of the quantum interference process in the presence of the SV field.

2. The Hamiltonian Model and the Equations of Motion

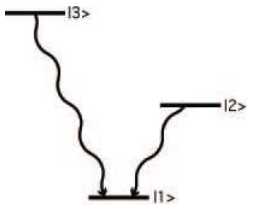

Figure 1: The V-system in the three-level atom

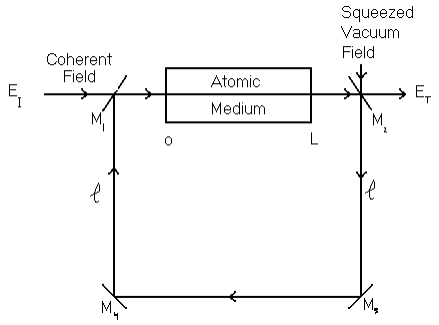

Figure 2: The ring cavity configuration

The 3-level atomic V-shape is schematically shown in Figure 1: The two-upper levels $|2>$ and $|3>$ (which couple by the same SV modes to the ground state $|1>$) decay to the single ground state $|1>$ – but the transition between $|2>$ and $|3>$ is not allowed. The Hamiltonian operator of the system is given by [15],

$$H = H_a \, + \, H_f \, + \, H_{af} \, , \tag{1}$$

where the atomic Hamiltonian H_a is given by,

$$H_a \, = \, \hbar \sum_{i=1}^{3} \omega_i \, S_{ii}, \tag{2a}$$

the free field Hamiltonian H_f is

$$H_f \, = \, \sum_{\underline{\kappa},\lambda} \omega_k \, a^{\dagger}_{\underline{\kappa},\lambda} \, a_{\underline{\kappa},\lambda} \tag{2b}$$

and the atom-field interaction Hamiltonian H_{af} is given by

$$H_{af} \, = \, \hbar \sum_{i=2}^{3} \left[\sum_{\underline{\kappa},\lambda} g_{i,\underline{\kappa},\lambda} \, S_{i1} \, a_{\underline{\kappa},\lambda} \, - E_i \, e^{-i\nu t} S_{i1} \right] \, + \, h.c. \tag{2c}$$

The notations are: The atomic operators $S_{ij} = |i><j|$ obey the commutation algebra,

$$[S_{ij}, S_{k\ell}] \, = \, S_{i\ell} \, S_{jk} \, - \, S_{kj} \, S_{\ell i}.$$

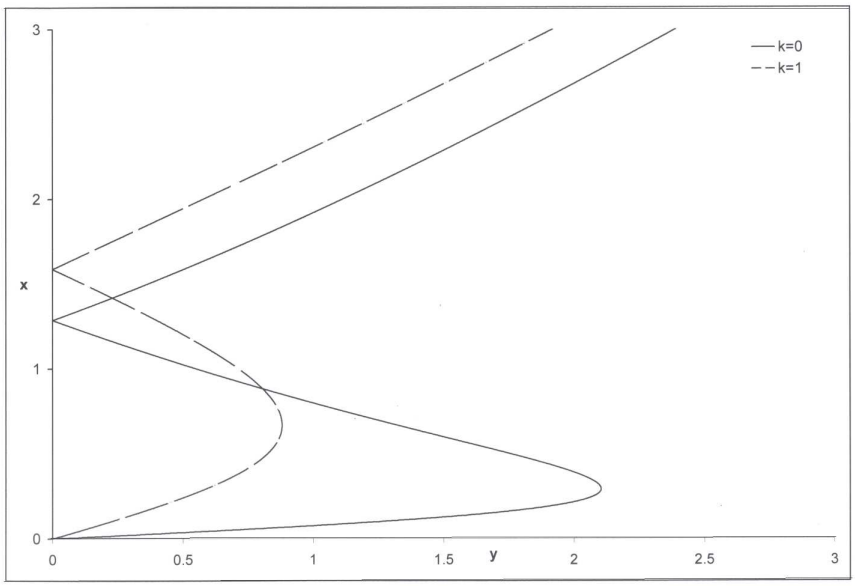

Figure 3: x versus y for $C = 5$, $\overline{\delta} = \overline{\Delta} = 0$, and $s = 0.5$ in the NV case

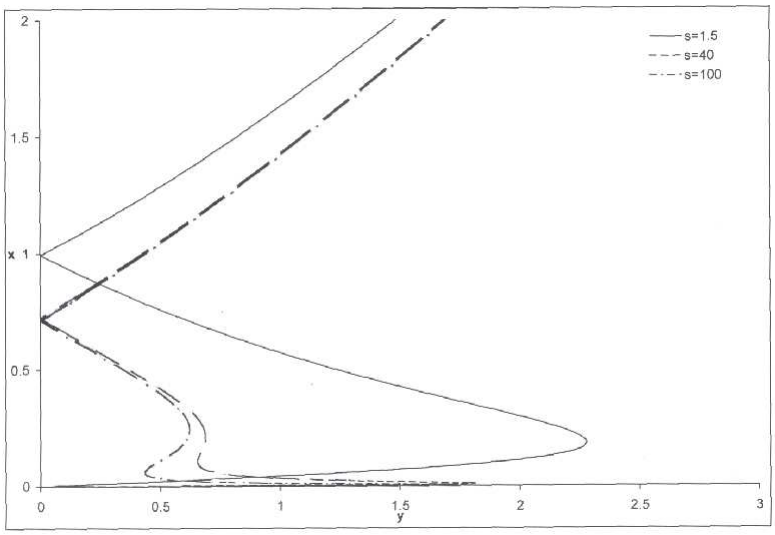

Figure 4: x versus y for $C = 5$, $\overline{\delta} = \overline{\Delta} = 0$ in the NV for various values of s

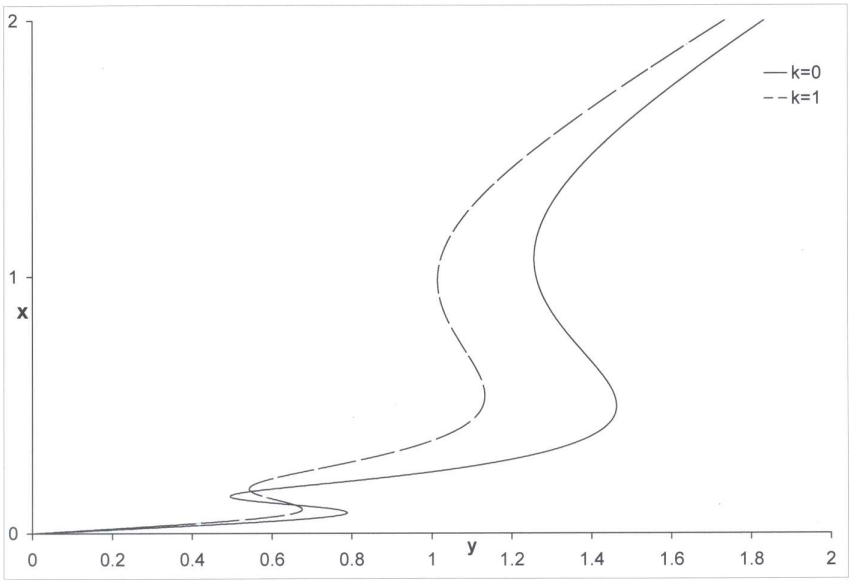

Figure 5: Same as Figure 3 but with $\overline{\delta} = 0.01$, $\overline{\Delta} = 0.3$ (resonance case)

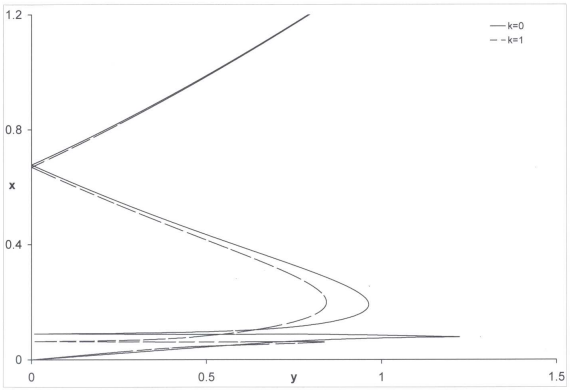

Figure 6: The resonance case for larger value of $n = 1$, $\phi = 0$, with $C = 5$ and $s = 100$

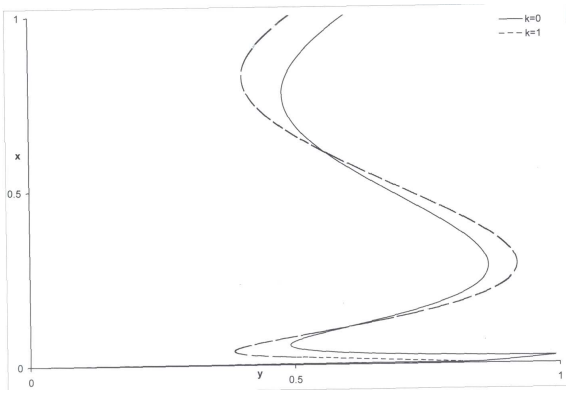

Figure 7: Multistability for both cases of k with $C = 5$, $s = 100$, $\overline{\delta} = 0.01$, $\overline{\Delta} = 0.3$ in the SV case $(n = 0.1, \phi = 0)$

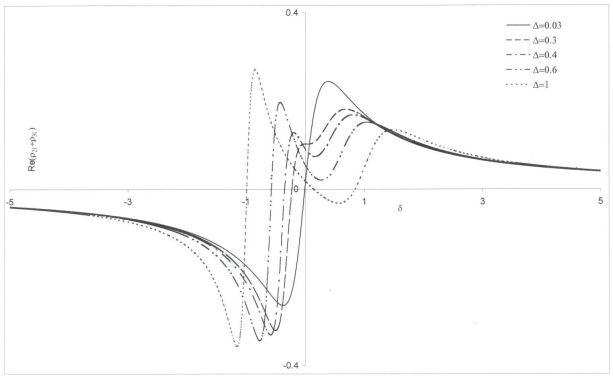

Figure 8: $\mathrm{Re}(\overline{\rho}_{21}+\overline{\rho}_{31})$ versus the detuning $\overline{\delta}$ for $k = 0$, $x = 0.1$, $s = 100$ and various values of $\overline{\Delta}$ in the NV case

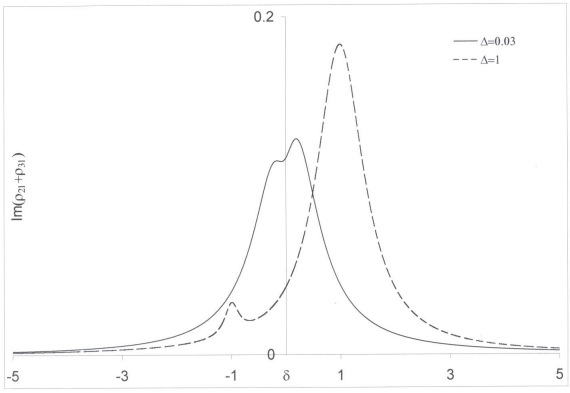

Figure 9: $\mathrm{Im}(\overline{\rho}_{21}+\overline{\rho}_{31})$ versus the detuning $\overline{\delta}$ for $k=0$, $x=0.1$, $s=100$ and various values of $\overline{\Delta}$ in the NV case

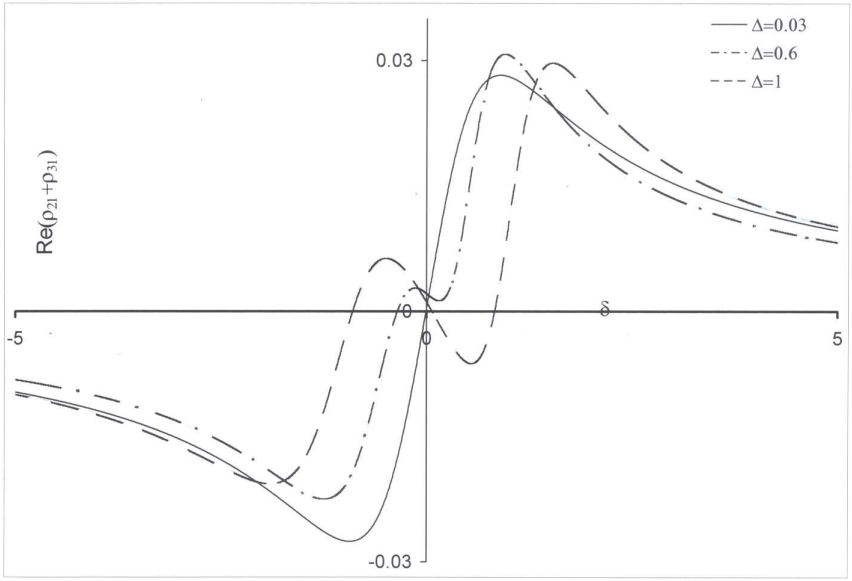

Figure 10a: $\mathrm{Re}(\overline{\rho}_{21}+\overline{\rho}_{31})$ versus the detuning $\overline{\delta}$ for $k=0$, $x=0.1$, $s=100$ and various values of $\overline{\Delta}$ in the SV case ($n=1$, $\phi=0$)

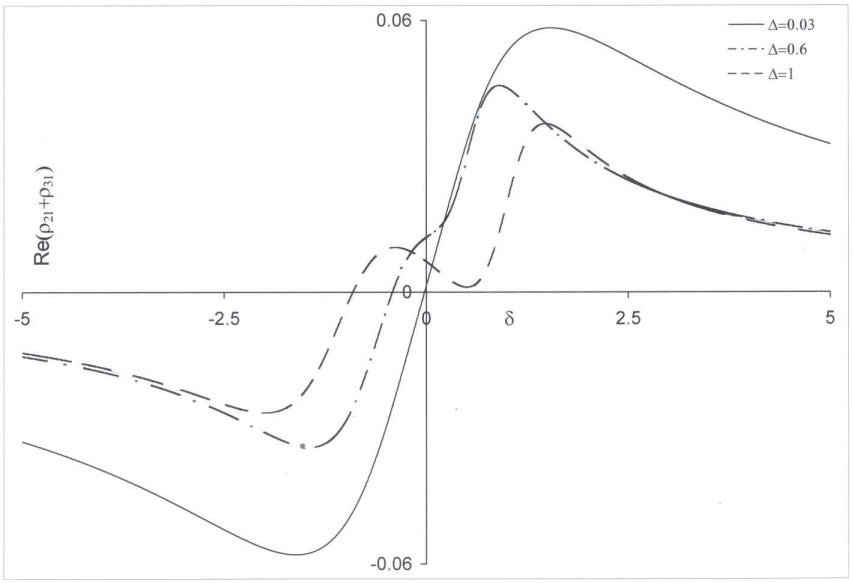

Figure 10b: Same as Figure 10a but for $k = 1$

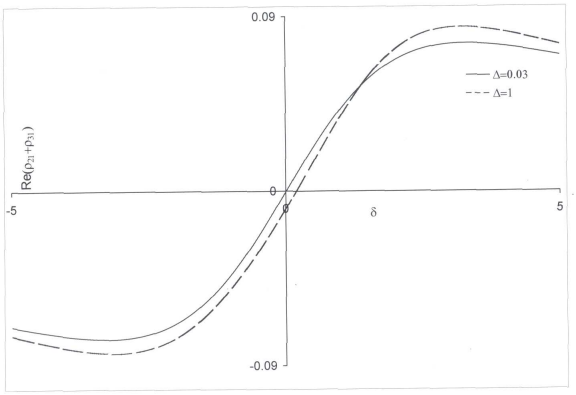

Figure 10b: $\mathrm{Re}(\overline{\rho}_{21} + \overline{\rho}_{31})$ versus the detuning $\overline{\delta}$ for $k = 0$, $x = 1$, $s = 2.25$ and various values of $\overline{\Delta}$ in the SV case ($n = 1$, $\phi = 0$)

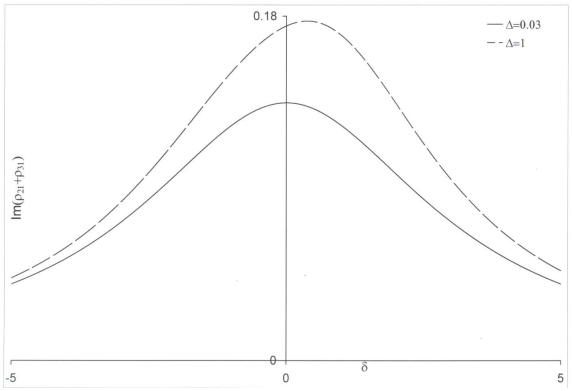

Figure 11a: $\mathrm{Im}(\overline{\rho}_{21} + \overline{\rho}_{31})$ versus the detuning $\overline{\delta}$ for $k = 0$, $x = 1$, $s = 2.25$ and various values of $\overline{\Delta}$ in the SV case ($n = 1$, $\phi = 0$)

The Boson Operators $a^{\dagger}_{\underline{\kappa},\lambda}$ and $a_{\underline{\kappa},\lambda}$ are the creation and annihilation operators of the field mode $(\underline{\kappa}, \lambda)$ ($\underline{\kappa}$ is the wave vector with polarisation index $\underline{\epsilon}_{\underline{\kappa},\lambda}$; $\lambda = 1, 2$) with algebra,

$$\left[a_{\underline{\kappa},\lambda},\, a^{\dagger}_{\underline{\kappa}',\lambda'}\right] \,=\, \delta_{\underline{\kappa},\underline{\kappa}'}\, \delta_{\lambda\lambda'}.$$

The coupling constant $g_{i,\underline{\kappa},\lambda} = \sqrt{\frac{\omega_k}{2\hbar V}}\, \underline{\mu}_{1i}.\underline{\epsilon}_{\underline{\kappa},\lambda}$ with V the quantisation volume, $\omega_k = kc$, $\kappa = |\underline{\kappa}|$ is the wave number, c =velocity of light and $\underline{\mu}_{1i}$ is the atomic dipole moment between the state $|1>$ and $|i>$; $i = 2, 3$; $E_i \equiv \hbar^{-1}\mu_{1i}E$ is the Rabi frequency of the transition $|i> \rightarrow |1>$ associated with the classical (laser) field of amplitude $E = E(z,t)$ and angular frequency ν. The resonant frequencies between the two upper states $|2>$, $|3>$ and the ground state $|1>$ are $\omega_{21} \equiv \omega_2 - \omega_1$ and $\omega_{31} \equiv \omega_3 - \omega_1$ respectively.

Following the operator approach [16,17], Heisenberg equation of motion for any atomic operator S_{ij}, $i\hbar\, S^{'}_{ij} = [S_{ij}, H]$, leads to the following equations of motion for the expectation value of the operators $\rho_{ij} =< S_{ij} >$ (where $< ... >$ means the quantum expectation value in the combined atom $\oplus$ field reservoir state) in normalised matrix form ($\tau = \sqrt{\gamma_2\, \gamma_3}\, t$

$$\frac{\partial}{\partial\tau}\,\overrightarrow{\overline{\rho}} = [A]\;\overrightarrow{\overline{\rho}} - \overrightarrow{B}\,, \tag{3}$$

where

$$[A] = \left[\begin{array}{cccc}
\xi_1 & -m\sqrt{s} & -\xi_2 & -k'\,m \\
-m^*\sqrt{s} & \xi_1^* & -k'\,m^* & \xi_2 \\
-\xi_2 & -k'\ m & \xi_3 & -m\,\sqrt{s} \\
-k'\,m^* & -{\xi^*}_2 & -\ m^*\sqrt{s} & {\xi^*}_3 \\
\frac{i\mu}{\hbar\sqrt{\gamma_2\gamma_3}}\overline{E} & \frac{-i\mu}{\hbar\sqrt{\gamma_2\gamma_3}}\overline{E}^* & 0 & 0 \\
0 & 0 & \frac{i\mu'}{\hbar\sqrt{\gamma_2\gamma_3}}\overline{E} & \frac{-i\mu'}{\hbar\sqrt{\gamma_2\gamma_3}}\overline{E}^* \\
0 & \frac{-i\mu'}{\hbar\sqrt{\gamma_2\gamma_3}}\overline{E}^* & \frac{i\mu}{\hbar\sqrt{\gamma_2\gamma_3}}\overline{E} & 0 \\
\frac{i\mu'}{\hbar\sqrt{\gamma_2\gamma_3}}\overline{E} & 0 & 0 & \frac{-i\mu}{\hbar\sqrt{\gamma_2\gamma_3}}\overline{E}^*
\end{array}\right.$$

$$\left.\begin{array}{cccc}
\frac{2\,i\mu}{\hbar\sqrt{\gamma_2\gamma_3}}\overline{E}^* & \frac{i\mu}{\hbar\sqrt{\gamma_2\gamma_3}}\overline{E}^* & 0 & \frac{i\mu'}{\hbar\sqrt{\gamma_2\gamma_3}}\overline{E}^* \\
\frac{-2\,i\mu}{\hbar\sqrt{\gamma_2\gamma_3}}\overline{E} & \frac{-\,i\mu}{\hbar\sqrt{\gamma_2\gamma_3}}\overline{E} & \frac{-\,i\mu'}{\hbar\sqrt{\gamma_2\gamma_3}}\overline{E} & 0 \\
\frac{i\mu'}{\hbar\sqrt{\gamma_2\gamma_3}}\overline{E}^* & \frac{2\,i\mu'}{\hbar\sqrt{\gamma_2\gamma_3}}\overline{E}^* & \frac{i\mu}{\hbar\sqrt{\gamma_2\gamma_3}}\overline{E}^* & 0 \\
\frac{-i\mu}{\hbar\sqrt{\gamma_2\gamma_3}}\overline{E} & \frac{-2i\mu}{\hbar\sqrt{\gamma_2\gamma_3}}\overline{E} & 0 & \frac{-i\mu}{\hbar\sqrt{\gamma_2\gamma_3}}\overline{E} \\
-\sqrt{s}\ (1+2\ n) & -\sqrt{s}\,n & \xi_2 & \xi_2 \\
-\frac{1}{\sqrt{s}}\,n & -\frac{1}{\sqrt{s}}(1+2\ n) & \xi_2 & \xi_2 \\
\xi_2 & \xi_2 & \xi_4 & 0 \\
\xi_2 & \xi_2 & 0 & \xi_4^*
\end{array}\right], \quad \text{(4 a)}$$

$$\overrightarrow{\rho} = \left[\ \rho_{12} \quad \rho_{21} \quad \rho_{13} \quad \rho_{31} \quad \rho_{22} \quad \rho_{33} \quad \rho_{23} \quad \rho_{32}\ \right]^T,$$

$$\overrightarrow{B} = \left[\ \frac{i\mu}{\hbar\sqrt{\gamma_2\gamma_3}}\overline{E}^* \quad \frac{-i\mu}{\hbar\sqrt{\gamma_2\gamma_3}}\overline{E} \quad \frac{i\mu'}{\hbar\sqrt{\gamma_2\gamma_3}}\overline{E}^* \quad \frac{-i\mu'}{\hbar\sqrt{\gamma_2\gamma_3}}\overline{E} \right.$$

$$\left. -\sqrt{s}\,n \quad -\tfrac{1}{\sqrt{s}}\,n \quad -k'n \quad -k'n\ \right]^T. \quad \text{(4 b)}$$

The "bar" notation in (3) and (4) means space average: $\overline{\rho}_{ij}(t) = L^{-1}\int_0^L \rho_{ij}(z,t)dz$, $\overline{E}(t) = L^{-1}\int_0^L E(z,t)dz$, and have used the mean field approximation [9, 13, 18] for the bilinear terms: $\overline{\rho_{ij}(z,t)E(z,t)} \approx \overline{\rho}_{ij}(t)\,\overline{E}(t)$. The symbols in (4a) are

$$\begin{aligned}
\overline{\xi}_1 &= i(\overline{\delta} - \overline{\Delta})\sqrt{s} - \frac{1}{2}\ (1+2\ n)\,\sqrt{s} - \frac{n}{2}\ \frac{1}{\sqrt{s}}\,, \\
\overline{\xi}_2 &= \frac{1+\ n}{2}\ \kappa', \qquad \kappa' = \kappa/2\,, \\
\overline{\xi}_3 &= i(\overline{\delta} + \overline{\Delta})\sqrt{s} - \frac{n}{2}\ \sqrt{s} - \frac{1}{2}\ (1-2\ n)\ \frac{1}{\sqrt{s}}\,, \\
\overline{\xi}_4 &= 2\ i\ \overline{\Delta}\sqrt{s} - \frac{1+\ n}{2}\ \left(\sqrt{s} + \frac{1}{\sqrt{s}}\right), \qquad (5)
\end{aligned}$$

$s = \frac{\gamma_2}{\gamma_3}$, $\overline{\Delta} = \frac{\Delta}{\gamma_2}$, $\overline{\delta} = \frac{\delta}{\gamma_2}$, $\Delta = \omega_2 - \omega_3$, and $\delta = 2\nu - \omega_2 - \omega_3$, where ν is the coherent field frequency, and n, $m = |m| \exp(i\phi)$ are the squeezed vacuum field reservoir parameters ($|m|^2 \leq n(n+1)$) [16, 17]. The constant $\gamma_i = \frac{3}{4}\mu_{i1}^2 \hbar^{-1} \omega_{i1}^3 / c^3$ $(i = 2, 3)$ is the decay rate of the excited state $|i>$ to the ground state $|1>$, $\mu_{i1} = |\underline{\mu}_{i1}|$ and the parameter κ is defined through: $\gamma_{23} = \frac{1}{2}\sqrt{\gamma_2 \gamma_3}\left(\frac{\underline{\mu}' \cdot \underline{\mu}}{\underline{\mu}' \underline{\mu}}\right) \equiv \frac{\kappa}{2}\sqrt{\gamma_2 \gamma_3}$, a measure of the quantum interference effect ($\kappa = 1$ corresponds to maximum interference when the transition moments $\underline{\mu} \equiv \underline{\mu}_{21}$ and $\underline{\mu}' \equiv \underline{\mu}_{31}$ are parallel, $\kappa = 0$ corresponds to no interference effect when $\underline{\mu}$ and $\underline{\mu}'$ are orthogonal).

In the absence of the SV field ($n = m = 0$) equation (3) and equation (4) reduce to those derived in the NV case [18].

3. Steady States Solutions

In the steady state ($\frac{\partial}{\partial \tau} \overrightarrow{\overline{\rho}}_{ij} = 0$) the system (3) gives the formal solutions for the matrix elements $\overline{\rho}_{ij}$

$$\overrightarrow{\overline{\rho}} = [A]^{-1} \overrightarrow{B}. \tag{6}$$

Further, Maxwell's equation in the steady state for the cavity field envelope $E(z)$ is of the form [18]

$$c\frac{\partial E}{\partial z} = -2\pi\, i\, \nu\; N\mu(\rho_{21}(z) + \rho_{31}(z))\,, \tag{7}$$

where N is the atomic density and have taken $\mu = \mu'$. In the ring cavity configuration (Figure 2) the boundary conditions (BC) for the cavity field $E(z)$ in the steady state limit are [13],

$$E(0) = \sqrt{T}\, E_I \;+\; R\, E(L)\, exp(-i\theta T), \quad E(L) = \frac{E_T}{\sqrt{T}}\,, \tag{8}$$

where $\theta = (\omega_c - \omega_d)/k_0$ is the normalised cavity detuning parameter, ω_c is the frequency of the cavity mode and ω_d is the frequency of the incident field and $k_0 = c/\mathcal{L}$ is the cavity decay rate, where $\mathcal{L} = 2(\ell + L)$ is the total length of the cavity.

Integrating equation (7) with the BC of (8) we get

$$E(L) - E(0) \quad = \quad -\frac{2\pi\, i\, \nu\, N\, \mu}{c} \int_0^L (\rho_{21}(z) + \rho_{31}(z))dz$$

$$= \quad -\frac{2\pi\, i\, \nu\, N\, L\, \mu}{c}(\overline{\rho}_{21} + \overline{\rho}_{31})\,, \tag{9}$$

where the steady state space averaged quantity $(\overline{\rho}_{21} + \overline{\rho}_{31})$ is obtained from (6), where the steady state space averaged field $\overline{E}$ in the vector matrix $\overrightarrow{B}$ is to be replaced by $E(L)$ in the mean field limit [9, 13, 18].

From equation (9) we get the steady state characterestic input-output relation in the form

$$y = x + iC\ (\overline{\rho}_{21} + \overline{\rho}_{31})\,, \tag{10}$$

where $C = \frac{2\ \pi\ \nu\ N\mu^2}{\hbar\gamma_2\ cT}$ is the cooperative parameter, $x = \frac{\mu E_T}{\hbar\ \gamma_2\sqrt{T}} = |x|$ and $y = \frac{\mu E_I}{\hbar\ \gamma_2\sqrt{T}}$ are the normalised real output and input fields respectively and have taken $\gamma_3 = \gamma_2$.

4. Computational Results

4.1. Input-Output Relation

First we examine *the quantum interference effect ($k = 1$)* on the steady state relation, equation (10), and compare the results with the *non-interference* case ($k = 0$). To do so, The induced polarisation $(\overline{\rho}_{21} + \overline{\rho}_{31})$ is computed numerically from equations (6) for fixed values of the parameters C, $\overline{\delta}$, $\overline{\Delta}$, s, n, $|m| = \sqrt{n(n+1)}$ and ϕ.

In the NV case where $n = \phi = 0$ and for $C = 5$ at exact resonance ($\overline{\delta} = \overline{\Delta} = 0$) the system shows bistable behaviour in both cases of $k = 0, 1$; with larger bistable area and lower threshold on the former case (Figure 3). Increasing the ratio of the two decay channels $s = (\gamma_2/\gamma_3)$ shows a multistable behaviour (indeed double bistable behaviour) only in the no-quantum interference case, $k = 0$ (no effect is noticed for $k = 1$), (Figure 4). In the off-resonance case ($\overline{\delta}, \overline{\Delta} \neq 0$), the multistable behaviour occurs in both cases of $k = 0, 1$ (Figure 5) with switching-down values of the input field y occuring at larger values relative to the resonance case (Figure 3 and Figure 4).

In the SV case ($n = 0.1$, $\phi = 0$) and for $C = 5$ at exact resonance the system shows multistable behaviour in both cases ($k = 0, 1$), Figure 6, compared with the NV case of Figure 4 where nultistable behaviour occurs only for $k = 0$. In the off-resonance case ($\overline{\Delta}, \overline{\delta} \neq 0$) both cases of $k = 0, 1$ show multistable behaviour, Figure 7-but SV parameters have the effect of reducing the difference between the two switching-on values in the case $k = 0$ compared with the NV case (Figure 5).

4.2. Susceptibility Response

Here, we examine the real and imaginary parts of susceptibility which is propotional to the induced polarisation $(\overline{\rho}_{21} + \overline{\rho}_{31})$ as a function of the normalised detuning parameter $\overline{\delta}$ at fixed values of the output field x.

In the NV case ($n = m = 0$) and for $|x| = 0.1$ and $s = 10$, the dispersive behaviour which is governed by $\mathrm{Re}(\overline{\rho}_{21} + \overline{\rho}_{31})$ in the case $k = 0$ has the usual dispersive curve (symmetric with respect to origion $\overline{\delta} = 0$) for $\overline{\Delta} = 0$ but loses symmetry for $\overline{\Delta}$: the dispersive curve shifts to the left until for $\overline{\Delta} \approx 0.4$ where it shows pronounced asymmetry in its positive part (Figure 8). In the interfernce case ($k = 1$) and for the same set of parameters we have similar qualitative behaviour but with higher peak values. The absorptive behaviour which is governed by $\mathrm{Im}(\overline{\rho}_{21} + \overline{\rho}_{31})$ shows that in the $k = 0$ case (Figure 9) the slightly dip structure around $\overline{\delta} = 0$ for $\overline{\Delta} = 0.03$ develops to a seperate peak at $\overline{\delta} = -1$ for $\overline{\Delta} = 1$. In the interference case $k = 1$ similar qualitative behaviour occurs but with no dip structure for $\overline{\Delta} = 0.03$.

In the SV case ($n = 1$, $\phi = 0$) extra resonances occur in $\mathrm{Re}(\overline{\rho}_{21} + \overline{\rho}_{31})$ for both cases of $k = 0, 1$ (Figure 10a and Figure 10b) as $\overline{\Delta}$ increases: $\overline{\Delta} \approx 0.6$ and 1respectively are the critical values to shift from the symmetric dispersive curve to the asymmetric curve. As for the absorptive behaviour, $\mathrm{Im}(\overline{\rho}_{21} + \overline{\rho}_{31})$, we have similar qualitative behaviour in both cases of $k = 0, 1$ to that of the NV case of Figure 9-except that no dip structure in the case of $k = 0$ and $\overline{\Delta} = 0.03$. For larger value of the output field $x = 1$ and smaller value of $s = 2.25$ the extra resonance structure (causing asymmetry) disappears in the dispersive and absorptive behaviour of the susceptibility for $k = 0$ (Figure 11a and Figure 11b)-similarly for $k = 1$

5. Conclusion

The OB model of atomic medium of 3-level V-shaped structure placed in a ring cavity and in contact with a phase sensitive reservoir (SV field) is investigated in the mean field limit and in the steady state case. The combined role of the quantum interference effect and the SV field is discussed for the susceptibility response function. Our main computational results are:

(i) The input-output field relation shows multi-stable behaviour if both quantum interference and SV field (with suitable SV phase value) effects are taken into account. Effect of increasing the ratio of the two decay channel rates of the two upper levels induces bi-stable behaviour in the input-output curve

in the NV case with no quantum interference effect at exact resonance.

(ii) The frequency mismatch between the two upper levels causes asymmetry in both the absorptive and dispersive nature of the susceptibility response function. Increasing this frequency mismatch induces additional resonance for (small) fixed output field with more asymmetry due to quantum interference effect. The enhanced dispersion (Figure 10a) is due to the presence of the SV field which in turn causes redistribution of the noise surrounding the atomic medium as well as the consideration of the quantum interference which overcomes the spontaneous relaxation of atomic coherence [18] leads too to higher extremal values of the dispersive part of the susceptibility response function for small atomic frequency mismatch.

Acknowledgments

The author is grateful to the University Research Committee of King Abdul Aziz University for their financial support (project N.422/504). Thanks, also, to Professor S.S. Hassan of University of Bahrain for his valuable comments and constructive suggestions and consultation throughout the investigation of this paper.

References

[1] R.L. Sutherland, *Handbook of Nonlinear Optics*, Marcel Dekker Inc., N.Y. (1996).

[2] B.S. Wherrett, P. Chavel, Ed-s, *Optical Computing*, Inst. Of Physics Publ., Bristol (1995).

[3] J.N. Lee, Ed., *Design Issues in Optical Processing*, Cambridge Univ. Press, Cambridge, U.K. (1995).

[4] D.G. Feitelson, *Optical Computing*, MIT Press, Mass, (1988).

[5] P. Mandel, *Theoretical Problems in Cavity Nonlinear Optics*, Cambridge Univ. Press, Cambridge, U.K. (1997).

[6] L.A. Lugiato, L.M. Narducci, In: *Fundamental Systems in Quantum Optics* (Ed-s: J. Dalibard, J.M. Raimond, J. Zinn-Justin), Elsevier Sci. Publ., Amesterdam (1992), 942-1043.

[7] *Physics World*, Volume **14** (April 2002), 21.

[8] V.V. Dodonov, *J. Opt. B: Quantum Semiclass. Opt.*, **4**, R1 (2002).

[9] R. Bonifacio, L.A. Lugiato, *Opt. Comm.*, **19**, No. 172 (1976).

[10] S.F. Hass, M. Sargent III, *Opt. Comm.*, **79**, No. 366 (1990).

[11] P. Galatola, L.A. Lugiato, M. Porreca, P. Tombsi, *Opt. Comm.*, **81**, No. 175 (1991).

[12] J. Bergou, D. Zhao, *Phys. Rev. A*, **52**, No. 1550 (1995).

[13] S.S. Hassan, H.A. Batarfi, R. Saunders, R.K. Bullough, *Euro. Phys. J. D.*, **8**, No. 403 (2000).

[14] H.A. Batarfi, S.S. Hassan, R. Saunders, R.K. Bullough, *Euro. Phys. J.D.*, **8**, No. 417 (2000).

[15] M.O. Scully, M.S. Zubairy, *Quantum Optics*, Cambridge Univ. Press, Cambridge, U.K. (1997).

[16] S.S. Hassan, H.A. Batarfi, R.K. Bullough, *J. Opt. B: Quantum Semiclass. Opt.*, **2**, R35 (2000).

[17] S.S. Hassan, M.R. Wahiddin, R. Saunders, R.K. Bullough, *Physica A*, **215**, No. 556; ibid. **219**, No. 482 (1995).

[18] M.A. Anton, O.G. Calderon, *J. Opt. B: Quantum Semiclass. Opt.*, **4**, No. 91 (2002).